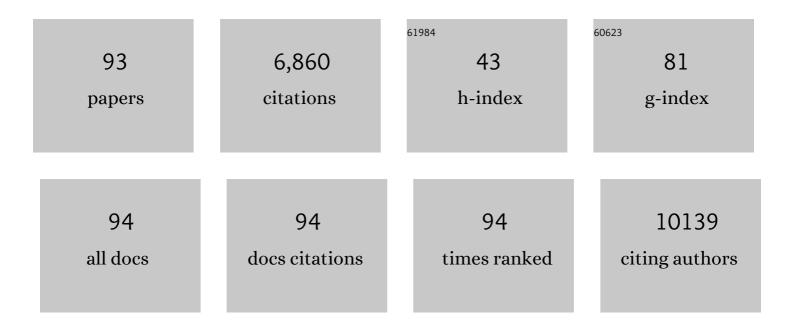
List of Publications by Year in descending order

Source: https://exaly.com/author-pdf/5241253/publications.pdf Version: 2024-02-01



DE-HULL

| #  | Article  | IF   | CITATIONS |
|----|--|------|-----------|
| 1  | Flexible capacitive pressure sensors for wearable electronics. Journal of Materials Chemistry C, 2022, 10, 1594-1605.  | 5.5  | 82        |
| 2  | Optical characteristics of self-trapped excitons in 2D (iso-BA) <sub>2</sub> PbI <sub>4</sub> perovskite crystals. Photonics Research, 2022, 10, 594.  | 7.0  | 6         |
| 3  | Nonvolatile electrical switching of optical and valleytronic properties of interlayer excitons. Light:<br>Science and Applications, 2022, 11, 23.  | 16.6 | 9         |
| 4  | Site-controlled interlayer coupling in WSe2/2D perovskite heterostructure. Science China Materials, 2022, 65, 1337-1344.   | 6.3  | 8         |
| 5  | Enhanced Rashba Indirect Exciton Emission in 2D Dion–Jacobson Perovskite Microplates via Efficient<br>Photon Recycling. Advanced Optical Materials, 2022, 10, 2102103.                       | 7.3  | 3         |
| 6  | Artificial Synapses Based on WSe <sub>2</sub> Homojunction via Vacancy Migration. ACS Applied<br>Materials & Interfaces, 2022, 14, 21141-21149.  | 8.0  | 12        |
| 7  | Enhancing Self-Trapped Exciton Emission via Energy Transfer in Two-Dimensional/Quantum Dot<br>Perovskite Heterostructures. ACS Photonics, 2022, 9, 2008-2014.                                | 6.6  | 11        |
| 8  | Light-Controlled Reconfigurable Optical Synapse Based on Carbon Nanotubes/2D Perovskite<br>Heterostructure for Image Recognition. ACS Applied Materials & Interfaces, 2022, 14, 28221-28229. | 8.0  | 6         |
| 9  | Giant enhancement of photoluminescence quantum yield in 2D perovskite thin microplates by graphene encapsulation. Nano Research, 2021, 14, 1980-1984.  | 10.4 | 9         |
| 10 | Recent Progress in Short―to Longâ€Wave Infrared Photodetection Using 2D Materials and<br>Heterostructures. Advanced Optical Materials, 2021, 9, 2001708.                                     | 7.3  | 118       |
| 11 | 2D perovskite narrowband photodetector arrays. Journal of Materials Chemistry C, 2021, 9, 11085-11090.   | 5.5  | 18        |
| 12 | Epitaxial growth of CsPbBr3-PbS vertical and lateral heterostructures for visible to infrared broadband photodetection. Nano Research, 2021, 14, 3879-3885.                                  | 10.4 | 25        |
| 13 | Seedsâ€Assisted Spaceâ€Confined Growth of Allâ€Inorganic Perovskite Arrays for Ultralowâ€Threshold<br>Singleâ€Mode Lasing. Laser and Photonics Reviews, 2021, 15, 2000428.                   | 8.7  | 24        |
| 14 | Recent progress in two-dimensional Ruddlesden–Popper perovskite based heterostructures. 2D<br>Materials, 2021, 8, 022006.  | 4.4  | 19        |
| 15 | Exciton–Phonon Interaction-Induced Large In-Plane Optical Anisotropy in Two-Dimensional<br>All-Inorganic Perovskite Crystals. Journal of Physical Chemistry Letters, 2021, 12, 3387-3392.    | 4.6  | 15        |
| 16 | Thermally Assisted Rashba Splitting and Circular Photogalvanic Effect in Aqueously Synthesized 2D<br>Dion–Jacobson Perovskite Crystals. Nano Letters, 2021, 21, 4584-4591.                   | 9.1  | 22        |
| 17 | Recent Progress of Chiral Perovskites: Materials, Synthesis, and Properties. Advanced Materials, 2021, 33, e2008785.   | 21.0 | 126       |
| 18 | Self-Powered Filterless On-Chip Full-Stokes Polarimeter. Nano Letters, 2021, 21, 6156-6162.  | 9.1  | 13        |

| #  | Article   | IF   | CITATIONS |
|----|---|------|-----------|
| 19 | Two-Dimensional Hybrid Perovskite-Based van der Waals Heterostructures. Journal of Physical<br>Chemistry Letters, 2021, 12, 8178-8187.  | 4.6  | 18        |
| 20 | Roomâ€Temperature Excitonâ€Based Optoelectronic Switch. Small, 2021, 17, e2005918.  | 10.0 | 11        |
| 21 | Full‣tokes Polarimeter Based on Chiral Perovskites with Chirality and Large Optical Anisotropy.<br>Small, 2021, 17, e2103855.   | 10.0 | 23        |
| 22 | Halide perovskites: from materials to optoelectronic devices. Frontiers of Optoelectronics, 2020, 13, 191-192.  | 3.7  | 4         |
| 23 | Robust Interlayer Coupling in Two-Dimensional Perovskite/Monolayer Transition Metal<br>Dichalcogenide Heterostructures. ACS Nano, 2020, 14, 10258-10264.  | 14.6 | 67        |
| 24 | Manipulation of Valley Pseudospin by Selective Spin Injection in Chiral Two-Dimensional<br>Perovskite/Monolayer Transition Metal Dichalcogenide Heterostructures. ACS Nano, 2020, 14,<br>15154-15160.                     | 14.6 | 49        |
| 25 | Self-trapped excitons in two-dimensional perovskites. Frontiers of Optoelectronics, 2020, 13, 225-234.  | 3.7  | 77        |
| 26 | Large Optical Anisotropy in Two-Dimensional Perovskite<br>[CH(NH <sub>2</sub> ) <sub>2</sub> ][C(NH <sub>2</sub> ) <sub>3</sub> ]PbI <sub>4</sub> with<br>Corrugated Inorganic Layers. Nano Letters, 2020, 20, 2339-2347. | 9.1  | 40        |
| 27 | Reversible luminescent humidity chromism of organic–inorganic hybrid<br>PEA <sub>2</sub> MnBr <sub>4</sub> single crystals. Dalton Transactions, 2020, 49, 5662-5668.   | 3.3  | 65        |
| 28 | Electric-field-induced phase transition in 2D layered perovskite (BA)2PbI4 microplate crystals. Applied<br>Physics Letters, 2020, 116, .  | 3.3  | 4         |
| 29 | The strain effects in 2D hybrid organic–inorganic perovskite microplates: bandgap, anisotropy and stability. Nanoscale, 2020, 12, 6644-6650.  | 5.6  | 15        |
| 30 | Biexcitons in 2D (iso-BA) <sub>2</sub> PbI <sub>4</sub> perovskite crystals. Nanophotonics, 2020, 9,<br>2001-2006.  | 6.0  | 19        |
| 31 | Circularly Polarized Luminescence from Chiral Tetranuclear Copper(I) Iodide Clusters. Journal of<br>Physical Chemistry Letters, 2020, 11, 1255-1260.  | 4.6  | 79        |
| 32 | Anisotropy of Excitons in Two-Dimensional Perovskite Crystals. ACS Nano, 2020, 14, 2156-2161.   | 14.6 | 52        |
| 33 | Optical anisotropy of one-dimensional perovskite<br>C <sub>4</sub> N <sub>2</sub> H <sub>14</sub> PbI <sub>4</sub> crystals. JPhys Photonics, 2020, 2,<br>014008.   | 4.6  | 16        |
| 34 | Photoinduced Trap Passivation for Enhanced Photoluminescence in 2D Organic–Inorganic Hybrid<br>Perovskites. Advanced Optical Materials, 2020, 8, 1901695.   | 7.3  | 14        |
| 35 | Multistate Memory Enabled by Interface Engineering Based on Multilayer Tungsten Diselenide. ACS<br>Applied Materials & Interfaces, 2020, 12, 58428-58434.   | 8.0  | 18        |
| 36 | Aqueous Synthesis of Low-Dimensional Lead Halide Perovskites for Room-Temperature Circularly<br>Polarized Light Emission and Detection. ACS Nano, 2019, 13, 9473-9481.  | 14.6 | 135       |

| #  | Article   | IF                               | CITATIONS           |
|----|---|----------------------------------|---------------------|
| 37 | Nonlinear optics of twoâ€dimensional transition metal dichalcogenides. InformaÄnÃ-Materiály, 2019, 1,<br>317-337.   | 17.3                             | 134                 |
| 38 | Light-Enhanced Ion Migration in Two-Dimensional Perovskite Single Crystals Revealed in Carbon<br>Nanotubes/Two-Dimensional Perovskite Heterostructure and Its Photomemory Application. ACS<br>Central Science, 2019, 5, 1857-1865.        | 11.3                             | 45                  |
| 39 | Reply to: Can lasers really refrigerate CdS nanobelts?. Nature, 2019, 570, E62-E64.   | 27.8                             | 4                   |
| 40 | Filterless Polarizationâ€Sensitive 2D Perovskite Narrowband Photodetectors. Advanced Optical<br>Materials, 2019, 7, 1900988.  | 7.3                              | 83                  |
| 41 | Chargeâ€Accumulation Effect in Transition Metal Dichalcogenide Heterobilayers. Small, 2019, 15, e1902424.   | 10.0                             | 30                  |
| 42 | Surface depletion field in 2D perovskite microplates: Structural phase transition, quantum confinement and Stark effect. Nano Research, 2019, 12, 2858-2865.  | 10.4                             | 11                  |
| 43 | The Role of Chloride Incorporation in Leadâ€Free 2D Perovskite (BA) <sub>2</sub> SnI <sub>4</sub> :<br>Morphology, Photoluminescence, Phase Transition, and Charge Transport. Advanced Science, 2019, 6,<br>1802019.                      | 11.2                             | 42                  |
| 44 | High-Performance Photodetectors Based on Lead-Free 2D Ruddlesden–Popper<br>Perovskite/MoS <sub>2</sub> Heterostructures. ACS Applied Materials & Interfaces, 2019, 11,<br>8419-8427.  | 8.0                              | 114                 |
| 45 | A field-effect approach to directly profiling the localized states in monolayer MoS2. Science Bulletin, 2019, 64, 1049-1055.  | 9.0                              | 5                   |
| 46 | Nonlayered Two-Dimensional Defective Semiconductor γ-Ga <sub>2</sub> S <sub>3</sub> toward<br>Broadband Photodetection. ACS Nano, 2019, 13, 6297-6307.  | 14.6                             | 72                  |
| 47 | Giant Nonlinear Optical Response in 2D Perovskite Heterostructures. Advanced Optical Materials, 2019, 7, 1900398.   | 7.3                              | 58                  |
| 48 | Controllable Growth of Centimeter-Sized 2D Perovskite Heterostructures for Highly Narrow<br>Dual-Band Photodetectors. ACS Nano, 2019, 13, 5473-5484.  | 14.6                             | 110                 |
| 49 | Temperature-Dependent Band Gap in Two-Dimensional Perovskites: Thermal Expansion Interaction and Electron–Phonon Interaction. Journal of Physical Chemistry Letters, 2019, 10, 2546-2553.   | 4.6                              | 90                  |
| 50 | Chiral 2D Perovskites with a High Degree of Circularly Polarized Photoluminescence. ACS Nano, 2019,<br>13, 3659-3665.   | 14.6                             | 334                 |
| 51 | Recent progress of the optoelectronic properties of 2D Ruddlesden-Popper perovskites. Journal of Semiconductors, 2019, 40, 041901.  | 3.7                              | 17                  |
| 52 | Self-trapped state enabled filterless narrowband photodetections in 2D layered perovskite single<br>crystals. Nature Communications, 2019, 10, 806.   | 12.8                             | 207                 |
| 53 | Two-Dimensional Lead-Free Perovskite<br>(C <sub>6</sub> H <sub>5</sub> C <sub>2</sub> H <sub>4</sub> NH <sub>3</sub> ) <sub>2</sub> CsSn <sub>2<br/>with High Hole Mobility. Journal of Physical Chemistry Letters, 2019, 10, 7-12.</sub> | <td>b&gt;<i>7</i>37/sub&gt;</td> | b> <i>7</i> 37/sub> |
| 54 | Vaporâ€Phase Growth of CsPbBr <sub>3</sub> Microstructures for Highly Efficient Pure Green Light<br>Emission. Advanced Optical Materials, 2019, 7, 1801336.   | 7.3                              | 30                  |

| #  | Article   | IF   | CITATIONS |
|----|---|------|-----------|
| 55 | Fabrication of single phase 2D homologous perovskite microplates by mechanical exfoliation. 2D<br>Materials, 2018, 5, 021001.   | 4.4  | 65        |
| 56 | Controllable growth of two-dimensional perovskite microstructures. CrystEngComm, 2018, 20, 6538-6545.   | 2.6  | 14        |
| 57 | Two-Step Growth of 2D Organic–Inorganic Perovskite Microplates and Arrays for Functional Optoelectronics. Journal of Physical Chemistry Letters, 2018, 9, 4532-4538.                | 4.6  | 31        |
| 58 | Gate-Induced Insulator to Band-Like Transport Transition in Organolead Halide Perovskite. Journal of<br>Physical Chemistry Letters, 2017, 8, 429-434.                               | 4.6  | 20        |
| 59 | Controllable Synthesis of Two-Dimensional Ruddlesden–Popper-Type Perovskite Heterostructures.<br>Journal of Physical Chemistry Letters, 2017, 8, 6211-6219.                         | 4.6  | 54        |
| 60 | Chemical vapor deposition growth of single-crystalline cesium lead halide microplatelets and heterostructures for optoelectronic applications. Nano Research, 2017, 10, 1223-1233.  | 10.4 | 96        |
| 61 | The Effect of Thermal Annealing on Charge Transport in Organolead Halide Perovskite Microplate<br>Fieldâ€Effect Transistors. Advanced Materials, 2017, 29, 1601959.                 | 21.0 | 91        |
| 62 | Size-dependent phase transition in methylammonium lead iodide perovskite microplate crystals. Nature<br>Communications, 2016, 7, 11330.   | 12.8 | 206       |
| 63 | Electronic and Ionic Transport Dynamics in Organolead Halide Perovskites. ACS Nano, 2016, 10, 6933-6941.  | 14.6 | 115       |
| 64 | van der Waals Heterojunction Devices Based on Organohalide Perovskites and Two-Dimensional<br>Materials. Nano Letters, 2016, 16, 367-373.   | 9.1  | 185       |
| 65 | Reduced graphene oxide/silicon nanowire heterostructures with enhanced photoactivity and superior photoelectrochemical stability. Nano Research, 2015, 8, 2850-2858.                | 10.4 | 34        |
| 66 | Electric-field-induced strong enhancement of electroluminescence in multilayer molybdenum<br>disulfide. Nature Communications, 2015, 6, 7509.                                       | 12.8 | 132       |
| 67 | Toward Barrier Free Contact to Molybdenum Disulfide Using Graphene Electrodes. Nano Letters, 2015,<br>15, 3030-3034.  | 9.1  | 362       |
| 68 | Strain-induced spatially indirect exciton recombination in zinc-blende/wurtzite CdS<br>heterostructures. Nano Research, 2015, 8, 3035-3044.   | 10.4 | 14        |
| 69 | Wafer-scale growth of large arrays of perovskite microplate crystals for functional electronics and optoelectronics. Science Advances, 2015, 1, e1500613.                           | 10.3 | 265       |
| 70 | Quantum dots on vertically aligned gold nanorod monolayer: plasmon enhanced fluorescence.<br>Nanoscale, 2014, 6, 5592-5598.   | 5.6  | 53        |
| 71 | Solid-State Semiconductor Optical Cryocooler Based on CdS Nanobelts. Nano Letters, 2014, 14,<br>4724-4728.  | 9.1  | 22        |
| 72 | Electroluminescence and Photocurrent Generation from Atomically Sharp<br>WSe <sub>2</sub> /MoS <sub>2</sub> Heterojunction <i>p–n</i> Diodes. Nano Letters, 2014, 14,<br>5590-5597. | 9.1  | 937       |

| #  | Article  | IF   | CITATIONS |
|----|--|------|-----------|
| 73 | Nanocrystalline copper indium selenide (CuInSe2) particles for solar energy harvesting. RSC Advances, 2013, 3, 9829.   | 3.6  | 10        |
| 74 | Photoinduced Charge Transfer within Polyaniline-Encapsulated Quantum Dots Decorated on Graphene. ACS Applied Materials & amp; Interfaces, 2013, 5, 8105-8110.                              | 8.0  | 36        |
| 75 | Anisotropic deformation of Au nanoparticles by highly charged ion Xe <sup>21+</sup> irradiation.<br>Physica Scripta, 2013, T156, 014064.   | 2.5  | 1         |
| 76 | Laser cooling of a semiconductor by 40 kelvin. Nature, 2013, 493, 504-508.   | 27.8 | 264       |
| 77 | Vertically Aligned Gold Nanorod Monolayer on Arbitrary Substrates: Self-Assembly and Femtomolar<br>Detection of Food Contaminants. ACS Nano, 2013, 7, 5993-6000.                           | 14.6 | 218       |
| 78 | Demonstration of Net Laser Cooling in a Semiconductor. Asia-Pacific Physics Newsletter, 2013, 02, 27-28.   | 0.0  | 2         |
| 79 | Laser cooling of a semiconductor by 40 kelvin: an optical refrigerator based on cadmium sulfide nanoribbions. , 2013, , .  |      | 0         |
| 80 | Laser cooling of CdS nanobelts: Thickness matters. Optics Express, 2013, 21, 19302.  | 3.4  | 31        |
| 81 | Optical and Excitonic Properties of Crystalline ZnS Nanowires. , 2013, , 453-483.  |      | 0         |
| 82 | Optical and Electrical Properties of Wurtzite Copper Indium Sulfide Nanoflakes. Materials Express,<br>2012, 2, 344-350.  | 0.5  | 11        |
| 83 | Tailoring Optical Properties of Silicon Nanowires by Au Nanostructure Decorations: Enhanced Raman<br>Scattering and Photodetection. Journal of Physical Chemistry C, 2012, 116, 4416-4422. | 3.1  | 51        |
| 84 | Surface Depletion Induced Quantum Confinement in CdS Nanobelts. ACS Nano, 2012, 6, 5283-5290.  | 14.6 | 60        |
| 85 | Ordered Array of Gold Semishells on TiO <sub>2</sub> Spheres: An Ultrasensitive and Recyclable SERS Substrate. ACS Applied Materials & Interfaces, 2012, 4, 2180-2185.                     | 8.0  | 186       |
| 86 | Synthesis and optical properties of Ilâ $\in$ "VI 1D nanostructures. Nanoscale, 2012, 4, 1422.   | 5.6  | 74        |
| 87 | Electric-Field-Dependent Photoconductivity in CdS Nanowires and Nanobelts: Exciton Ionization,<br>Franz–Keldysh, and Stark Effects. Nano Letters, 2012, 12, 2993-2999.                     | 9.1  | 62        |
| 88 | Assembly of Colloidal Nanoparticles Directed by the Microstructures of Polycrystalline Ice. ACS Nano, 2011, 5, 8426-8433.  | 14.6 | 85        |
| 89 | A study of highly charged ions transmission through polycarbonate nanocapillaries with multi-holes.<br>Physica Scripta, 2011, T144, 014046.  | 2.5  | 3         |
| 90 | Flexible Visible–Infrared Metamaterials and Their Applications in Highly Sensitive Chemical and<br>Biological Sensing. Nano Letters, 2011, 11, 3232-3238.                                  | 9.1  | 215       |

| #  | Article   | IF  | CITATIONS |
|----|---|-----|-----------|
| 91 | Potential and Kinetic Electron Emissions from HOPG Surface Irradiated by Highly Charged Xenon and Neon Ions. Chinese Physics Letters, 2011, 28, 053402.         | 3.3 | 4         |
| 92 | Optical and Excitonic Properties of Crystalline ZnS Nanowires: Toward Efficient Ultraviolet Emission<br>at Room Temperature. Nano Letters, 2010, 10, 4956-4961. | 9.1 | 114       |
| 93 | Modulating the electronic structures of graphene by controllable hydrogenation. Applied Physics<br>Letters, 2010, 97, .   | 3.3 | 82        |